

**STRUCTURAL AND THERMAL TRANSITIONS DURING THE CONVERSION FROM  
NATIVE TO GRANULAR COLD-WATER SWELLING MAIZE STARCH**

**D.M. Dries<sup>1,3,\*</sup>, S.V. Gomand<sup>1,3</sup>, B. Goderis<sup>2,3</sup> and J.A. Delcour<sup>1,3</sup>**

<sup>1</sup>Laboratory of Food Chemistry and Biochemistry, KU Leuven, Kasteelpark Arenberg 20, B-

3001 Leuven, Belgium. E-mail: Sara.Gomand@biw.kuleuven.be;

Jan.Delcour@biw.kuleuven.be

<sup>2</sup>Polymer Chemistry and Materials, KU Leuven, Celestijnenlaan 200F, B-3001 Leuven,

Belgium. E-mail: Bart.Goderis@chem.kuleuven.be

<sup>3</sup>Leuven Food Science and Nutrition Research Centre (LFoRCe), KU Leuven, B-3001 Leuven,

Belgium

\*Corresponding author. Phone: (+32)-16-376776. Fax: (+32)-16-321997.

E-mail: Dorien.Dries@biw.kuleuven.be

**KEYWORDS:** starch; cold swelling; V-type crystallinity; X-ray diffraction; polarized optical  
microscopy; differential scanning calorimetry

**ABBREVIATIONS:** AP, amylopectin; AM, amylose; AML, amylose-lipid inclusion complex; CHL, carbohydrate leaching;  $T_{C(V)}$ , conclusion temperature of gelatinization (V-type crystal melting); DSC, differential scanning calorimetry;  $2\theta$ , diffraction angle; dm, dry matter;  $\Delta H_{(V)}$ , enthalpy of gelatinization (V-type crystal melting);  $ETS_{(waxy)x\%/y^{\circ}C}$ , ethanol treated (waxy) maize starch treated with x% (v/v) ethanol at a temperature of y °C; GCWSS, granular cold-water swelling starch;  $\Delta H_{AML}$ , amylose-lipid inclusion complex melting enthalpy;  $T_{O(V)}$ , onset temperature of gelatinization (V-type crystal melting);  $T_{P(V)}$ , peak temperature of gelatinization (V-type crystal melting); RT, room temperature;  $\Delta T_{(V)}$ , temperature range of gelatinization (V-type crystal melting); TGA, thermal gravimetric analysis;  $\lambda$ , wavelength; WAXD, wide angle X-ray diffraction

## ABSTRACT

Native maize starch was gradually converted into granular cold-water swelling starch (GCWSS) by aqueous ethanol treatments at elevated temperatures. At a treatment temperature of 95 °C, decreasing ethanol concentrations from 68 to 48% (v/v) led to decreased post-treatment gelatinization enthalpies in excess water, reflecting remaining original A-type crystals. Concomitantly to native A-type crystal melting, V<sub>H</sub>-type crystals appeared. At an ethanol concentration of 48%, a granular cold-water swelling maize starch was successfully produced. All crystals in its granules were of the V<sub>H</sub>-type and appeared birefringent when studied in ethanol under polarized light. Removal of all residual solvent by high temperature drying did not influence swelling power, proving that a high temperature drying step is not necessary to induce cold-water swelling capacity. Based on *in situ* calorimetric measurements, the thermal requirements to produce GCWSS from different ethanol:water mixtures were elucidated. This work is the first to demonstrate that the amylose fraction contributes almost exclusively to V<sub>H</sub>-type crystal formation in GCWSS.

## 1. INTRODUCTION

Native starch is laid down in plant storage organs as water insoluble, partly crystalline granules which essentially consist of two glucose polymers: quasi linear amylose (AM) and highly branched amylopectin (AP) (Buléon, Colonna, Planchot & Ball, 1998). Regions of AP double helical formation are embedded into crystalline lamellae which alternate with amorphous layers containing AP branching points (Jenkins, Cameron & Donald, 1993; Oostergetel & Vanbruggen, 1989). It is generally accepted that AM is located in the amorphous regions and that it does not participate in formation of crystals in native maize starch (Saibene & Seetharaman, 2010). The specific radial arrangement of starch crystallites gives rise to a Maltese cross pattern when the granules are visualized by optical microscopy in the polarization mode (French, 1984).

Differences in packing arrangements of AP double helices in native starch crystallites lead to characteristic A-, B- or C-type wide angle X-ray diffraction (WAXD) patterns (Imberty, Chanzy, Perez, Buleon & Tran, 1988; Imberty & Perez, 1988). A fourth pattern, the V-type, is the result of complexes of AM single helices with suitable ligands such as iodine, fatty acids and alcohols (Zobel, 1988). V<sub>H</sub>-type crystals are obtained in the case of saturated fatty acids and linear alcohols. Upon drying, an anhydrous V<sub>A</sub>-type diffraction pattern is obtained, which has the same general shape as the former but with reflections shifted towards larger Bragg angles (Le Bail, Bizot, Pontoire & Buleon, 1995). Although suitable ligands are necessary for forming AM single helical structures, their occurrence inside the helix cavity is not necessary for obtaining a V-type diffraction pattern (Le Bail, Bizot, Pontoire & Buleon, 1995; Whittam et al., 1989). As opposed to native A-, B- or C-starch crystals, V-type crystals can be soluble in water at room temperature (French & Murphy, 1977).

At room temperature, native starch granules remain virtually intact and precipitate from aqueous solutions. Starches with enhanced cold-water swelling capacity are used in puddings, pie

fillings, gravies, soups and sauces as thickening agents (Eastman, 1987). Such starches are traditionally prepared by drum drying gelatinized starch slurries (Colonna, Doublier, Melcion, Demonredon & Mercier, 1984; Doublier, Colonna & Mercier, 1986), but have inferior thickening properties due to their no longer being granular (Anastasiades, Thanou, Loulis, Stapatoris & Karapantsios, 2002). To overcome this limitation, some effort has been made to develop granular cold-water swelling starches (GCWSS). At industrial scales, native starch granules are often gelatinized in hot steam and nozzle-spray dried (Pitchon, O'Rourke & Joseph, 1981). According to Rajagopalan and Seib (1992b), this method yields amorphous GCWSS. Other technologies – the ones of interest to the present paper – make use of alcohols and produce GCWSS with increased levels of V-type crystallinity. These include (i) aqueous alcohol treatment at high temperature and elevated (Eastman, 1987; Eastman & Moore, 1984) or atmospheric pressure (Zhang, Dhital, Haque & Gidley, 2012) (method I), (ii) polyhydric alcohol (*e.g.* propan-1,2-diol) treatment at high temperature and atmospheric pressure (Rajagopalan & Seib, 1992a, b) (method II) and (iii) alcoholic-alkaline treatment (Chen & Jane, 1994a, b; Jane & Seib, 1991) (method III).

Jane *et al.* (1986a; 1986b) proposed a mechanism explaining the structural transitions during formation of GCWSS when prepared by method I in closed vessels at autogenic pressure. Rapidly after native crystal melting, the alcohol induces single helical formation and V-type crystallinity with the alcohol being located within the single helix cavities and possibly the interstices. This mechanism is supported by the observation that the endothermic heat of gelatinization in aqueous alcohol is lower than in pure water, supposedly since it is partially annihilated by the exothermic heat of V<sub>H</sub>-type crystal formation. Alcohol removal from the helix cavity by drying produces semi-stable V-type crystals and confers cold-water swelling capacity upon the starch (Jane, Craig, Seib & Hosene, 1986a). The integrity of the granules is thought to be preserved due to entanglement of AM with AP. This idea stems from the observation that the granular integrity could not be preserved in attempts to produce GCWSS of

waxy starch, which is free of AM. However, AP is believed to contribute to formation of V-type crystals since in WAXD experiments (Jane, Craig, Seib & Hoseney, 1986b) the intensity of the V-type diffraction pattern from regular GCWSS accounts for more than the AM fraction alone. To our opinion, this mechanism requires considerable extra research.

First of all, the thermal requirements to produce GCWSS by method I have never been fully unraveled. For instance, the work by Zhang *et al.* (2012) does not allow making clear statements on the role of different alcohol:water ratios at a treatment temperature of 95 °C because, in their method, the actual temperature drifted during the protocol, solvent evaporation occurred and hence the starch concentration progressively increased. Also, calorimetric measurements by Jane *et al.* (1986a) only included a single *n*-propanol:water solution and melting of created V-type crystals was not reported.

Secondly, the involvement of AP in V-type crystal formation, as proposed by Jane *et al.* (1986a), has never been confirmed. Chen and Jane (1994b) found no V-type crystallinity in GCWSS from waxy maize starch produced via method III. The granules remained amorphous. Zhang *et al.* (2012) used method I at ambient pressure. All GCWSS displayed V-type crystallinity except for partially converted waxy maize starches. The idea was coined that AM is needed for nucleation of V-type crystallinity and that AP can contribute once triggered by AM.

Finally, whether or not removal of alcohol is strictly needed to impart cold-water swelling properties remains undecided since – to the best of our knowledge – no solubility or swelling experiments were ever conducted on V-type crystalline GCWSS that did not pass a drying step in which the alcohol was removed.

The present work wants to contribute to the understanding of the GCWSS production process. It focuses on method I. Therefore, the first part of the current paper reports on a study in which the water:alcohol ratio and the treatment temperature – in a predefined temperature range up to 95 °C – are systematically varied. The properties of the ensuing products are fully characterized.

A second part discusses the importance of removing the alcohol from the V-type crystals for inducing cold-water swelling capacity. Alternative routes to produce GCWSS from the unsuccessful mixtures tested at 95 °C are proposed in a following part. This part provides clear answers on the temperature requirements for producing GCWSS by method I at a given water:alcohol ratio. Besides regular maize starch, waxy maize starch is included in this study to allow for a final discussion on the contribution of AP in the formation of V-type crystals.

## 2. EXPERIMENTAL SECTION

### 2.1 Materials

Normal and waxy maize starch were obtained from Cargill (Vilvoorde, Belgium). All reagents, solvents and chemicals were of at least analytical grade and obtained from Sigma-Aldrich (Bornem, Belgium). The ethanol used in this work is 5% diethyl ether-denaturated ethanol and will be further referred to as ethanol. This means more specifically that *e.g.* a stock solution of 48% (v/v) ethanol consists of 49.5% deionized water, 48% ethanol and 2.5% diethyl ether.

### 2.2 Procedure for preparing granular cold-water swelling starch on gram scale

GCWSS was produced by aqueous ethanol treatments at elevated temperature. The ethanol concentration ranged from 48 to 68% (v/v) and the treatment temperatures were 80, 85, 90, or 95 °C. Regular maize starch [20.0 g dry matter (dm) basis] (*cf.* §2.5) was suspended in a water:ethanol mixture [1/9 (w/w) starch dm/solvent] with varying ethanol concentration in a pressure resistant Schott bottle (250 ml) equipped with a leak proof screw cap. The bottles were hand shaken to disperse the starch and then continuously shaken in a water bath. After 30 min at the desired temperature, the suspensions were kept for 60 min at room temperature (RT), 200 ml ethanol was added and bottle contents were suspended. The starch suspensions were Büchner filtered and washed several times with ethanol. The resulting starch pellet was finely chopped with a spatula, spread over a paper filter sheet, air-dried overnight at RT, sieved (mesh size: 150 µm) and stored in air-tight plastic bottles. Sample codes are of the format ETS<sub>x%/y°C</sub> where ETS stands for ethanol treated starch, x% stands for the volume percentage of ethanol in the used water:ethanol mixture and y °C for the treatment temperature. The subscript 'waxy' is used when waxy instead of regular maize starch was used. An alternative treatment for overnight air-drying included oven-drying for 60 min at 115 °C (ETS<sub>x%/y°C\_115°C</sub>).

### 2.3 Differential Scanning Calorimetry

### *2.3.1 Gelatinization and amylose-lipid inclusion complex melting in excess water*

Gelatinization and amylose-lipid inclusion complex (AML) melting of native starch and ETS in excess water were studied with a Q2000 DSC (TA Instruments, New Castle, DE, USA). Starch samples (2.50-4.00 mg) were accurately weighed in an aluminum pan (Perkin-Elmer, Waltham, MA, USA) and deionized water was added [1/3 (w/w) starch dm/water]. The pans were hermetically sealed and heated from 20 to 120 °C at 4 °C/min. The gelatinization onset ( $T_O$ ), peak ( $T_P$ ) and conclusion ( $T_C$ ) temperatures, the temperature range ( $\Delta T$ ), gelatinization enthalpy ( $\Delta H$ ) and melting enthalpy of AML ( $\Delta H_{AML}$ ) were determined with TA Universal Analysis software. Empty pans were used as reference. Calibration was with indium. Analyses were performed at least in triplicate.

### *2.3.2 Gelatinization and V-type crystal melting in aqueous ethanol*

The aqueous ethanol treatments (*cf.* §2.2) were also executed in the DSC instrument. Native starch (about 2.25 mg) was accurately weighed in a high pressure steel pan (Mettler-Toledo, Zaventem, Belgium), water:ethanol mixture [68 to 48% (v/v) ethanol] was added [1/9 (w/w) starch dm/solvent] and the pans were hermetically sealed. Samples were heated from 20 to 180 °C at 4 °C/min. Their gelatinization characteristics were determined as outlined above. The V-type crystal melting onset ( $T_{O(V)}$ ), peak ( $T_{P(V)}$ ) and conclusion ( $T_{C(V)}$ ), melting range ( $\Delta T_{(V)}$ ) and melting enthalpy ( $\Delta H_{(V)}$ ) were determined as well. Instrument calibration and data analysis were as outlined above. Analyses were performed at least in duplicate. As a control, gelatinization of native maize starch in excess water [1/9 (w/w) starch dm/water] was also studied using high pressure steel pans.

## **2.4 Microscopy**

Light micrographs of native maize starch and ETS were taken in ethanol or deionized water with a Nikon (Melville, NY, USA) ECLIPSE 80i epifluorescence microscope equipped with a



charge-coupled device camera. Images were analyzed with NIS-Elements BR software (Nikon).  
The microscope was operated in bright field and polarization modes.

## 2.5 Chemical composition

Moisture contents of native and ETS were determined according to AACC approved method 44-15.02. Lipids of native starch and ETS were extracted with an accelerated solvent extractor and their contents determined gravimetrically as in Gerits *et al.* (2013). For the determination of AM content, native starch and ETS were first completely dispersed by heating in dimethyl sulfoxide. Lipid was then removed by precipitating the starch in 95% ethanol. This was done to avoid underestimation of AM contents due to presence of AM-lipid inclusion complexes. The precipitated starch was dispersed, AP was removed by precipitation with concanavalin A and AM was then subjected to amylolytic hydrolysis in the supernatant (Gibson, Solah & McCleary, 1997) using an AM/AP content assay kit (Megazyme, Wicklow, Ireland).

## 2.6 Swelling parameters

The close packing concentration ( $C^*$ ) is that at which swollen granules fill up the available space in a starch suspension (Eerlingen, Jacobs, Block & Delcour, 1997). Native maize starch and ETS were suspended in deionized water [0.011% (w/v)] in centrifuge tubes with screw caps. The tubes were placed in a water bath for 30 min at 20 °C with intermittent shaking every 5 minutes. The starch suspensions were centrifuged at 1000 g for 30 min. The supernatants were transferred to small test tubes and the sediments weighed.  $C^*$  (%) was calculated as follows:

$$C^* = \frac{\text{dry matter starch weight} \times 100}{\text{sediment weight}}$$

The swelling power (SP) is a measure of the water uptake by starch corrected for carbohydrate leaching (CHL) (Leach, Mccowen & Schoch, 1959). The level of soluble carbohydrates in the supernatant was determined after the close packing experiment by the method of Dubois *et al.*

(1956) using a glucose standard and expressing the leached carbohydrate as starch ( $0.9 \times$  glucose). SP (g/g) at 20 °C was calculated as follows:

$$SP = \frac{\text{sediment weight} \times 100}{\text{dry matter starch weight} \times (100 - \%CHL)}$$

## 2.7 Wide angle X-ray diffraction

Native starches and ETS were first equilibrated for 48 h in a humidifier to  $16 \pm 2\%$  final moisture content, enclosed in aluminum DSC pans (Perkin-Elmer) and sealed hermetically. Static WAXD measurements were performed with an XeuSS X-ray camera (Xenocs, Sassenage, France), comprising a GeniX 3D Molybdenum ultra-low divergence X-ray beam delivery system (wavelength,  $\lambda = 0.71 \text{ \AA}$ ) at a power of 50 kV – 1mA, a collimating assembly based on scatterless slits, a sample stage, a He flushed flight tube and a Mar345 image plate detector (MARresearch, Norderstedt, Germany). The scattering angles were calibrated using silver behenate and polyethylene. The 2D WAXD data were azimuthally averaged using the ConeX program (Gommes & Goderis, 2010). Intensity patterns were corrected for empty holder scattering, taking into account the sample and holder transmission. Transmissions were obtained by measuring the direct beam intensity with a photodiode placed downstream from the sample. The WAXD patterns were converted to the scattering angles  $2\theta$ , with  $\theta$  being half the scattering angle, as if Cu  $K_\alpha$  radiation ( $\lambda = 1.54 \text{ \AA}$ ) would have been used to facilitate comparison with literature data. The degree of crystallinity and proportions of A- and V<sub>H</sub>-type crystallinity were determined according to Cairns *et al.* (1997). An amorphous sample was prepared by freeze drying native maize starch, gelatinized in excess water. For each particular sample, a scaling factor was determined in order to fit the amorphous scattering pattern – in a predefined angular range of 5 to 27 °2θ (Cu  $K_\alpha$ ) – to the scattering pattern of the samples. The degree of crystallinity was calculated as follows:

$$\text{Degree of crystallinity (\%)} = \frac{I_s - (I_a \times fs)}{I_s} \times 100$$

with Is: integrated normalized intensity of the sample over the angular range 5 to 27 °2θ

Ia: integrated normalized intensity of an amorphous sample over the angular range 5 to 27 °2θ

fs: scaling factor corresponding to each particular sample

Subtracting the amorphous contributions ( $I_a \times f_s$ ) yielded scattering patterns accounting for the crystalline portion of the samples only. The resultant scattering patterns of waxy maize starch and GCWSS were taken to represent pure A and pure V<sub>H</sub> polymorphs. An appropriately proportioned combination of their scattering patterns was used to model (with a least-squares error fit) the scattering patterns of the samples and deduce proportions of A- and V<sub>H</sub>-type crystallinity (%). Note that a linear combination of the scattering patterns of the amorphous sample prepared as mentioned above and an amorphous sample dried at 115°C was used for the fitting procedure of ETS<sub>48%/95°C\_115°C</sub> and GCWSS produced on a mg scale (*cf.* §2.9).

## 2.8 Thermogravimetric analysis

Thermogravimetric analysis (TGA) of ETS<sub>48%/95°C</sub> was done using an auto TA Instruments TGA 2950. Measurements were performed under nitrogen atmosphere with a flow rate of 60 ml/min. About 6.00 mg of starch was accurately weighed for each test and samples were heated from 25 °C to 200 °C at 4 °C/min. Weight loss curves and first derivatives as a function of temperature were obtained using TA Universal Analysis Software. Analyses were performed in triplicate.

## 2.9 Procedure for preparing granular cold-water swelling starch on mg scale

Native starch (about 2.25 mg) was accurately weighed in a high pressure steel pan (Mettler-Toledo, Zaventem, Belgium) and water:ethanol mixtures – the ones that had proven to be unsuccessful at 95 °C [68, 58 and 53% (v/v) ethanol] – were added [1/9 (w/w) starch dm/solvent]. The pans were hermetically sealed and heated from 20 to 107, 112 or 133 °C, held at this temperature for 30 min and cooled to 20 °C in the DSC-instrument to obtain ETS<sub>53%/107°C</sub>, ETS<sub>58%/112°C</sub> and ETS<sub>68%/133°C</sub> respectively. The pans were opened, solvent was removed using a

Pasteur pipet, samples were washed several times with ethanol and air-dried overnight. The rationale behind using these treatment temperatures will be outlined in the discussion section.

## **2.10 Statistical analysis**

Statistical analyses were performed with Statistical Analysis System software 6.2 (SAS Institute, Cary, NC, USA). It was verified whether mean values were significantly ( $P < 0.05$ ) different using the one-way ANOVA procedure. Corresponding Tukey grouping coefficients are given.

### 3. RESULTS AND DISCUSSION

#### 3.1 Characterization of ethanol treated starch

##### 3.1.1 Gelatinization in excess water

The endothermic heat of starch gelatinization represents the energy that is needed for disruption of native molecular organization and is virtually zero for GCWSS (Jane, Craig, Seib & Hosney, 1986a; Zhang, Dhital, Haque & Gidley, 2012). Figure 1 represents the DSC gelatinization characteristics ( $T_O$ ,  $T_P$ ,  $T_C$ ,  $\Delta H$ ) of native (waxy) maize starch and ETS<sub>(waxy)</sub> in excess water. When the treatment temperature increased or the ethanol concentration decreased,  $\Delta H$  decreased and the residual starch melted at higher temperatures while  $\Delta T$  decreased. For instance, ETS<sub>58%/95°C</sub> had a lower  $\Delta H$  (6.4 J/g) and higher  $T_P$  (75.6 °C) than ETS<sub>58%/80°C</sub> ( $\Delta H$  = 14.4 J/g;  $T_P$  = 70.3 °C). Compared to ETS<sub>58%/95°C</sub>, lowering ethanol concentration by 5% (ETS<sub>53%/95°C</sub>) further reduced  $\Delta H$  (0.8 J/g) and increased  $T_P$  (81.0 °C). Finally, no detectable gelatinization endotherm was observed for ETS<sub>48%/95°C</sub>. Further lowering the ethanol concentration at this temperature led to formation of a starch gel. This indicated granule disruption. A similar trend was observed for ETS<sub>waxy</sub> (Figure 1).  $\Delta H$  of ETS<sub>waxy56%/95°C</sub> was approximately 7 J/g lower than that of native waxy maize starch. Unfortunately, it was not possible to find treatment parameters – within the predefined temperature range up to 95 °C – resulting in an ETS<sub>waxy</sub> showing no detectable DSC endotherm without starch granule disruption. In what follows, starches treated at 95 °C at different ethanol concentrations – which cover a range of ETS with gelatinization characteristics from approximately native starch up to a point where no endothermic heat of gelatinization could be observed – are further characterized.

##### 3.1.2 Granular morphology

Figure 2 shows bright field (A1-E1) and polarized light (A2-E2) micrographs of native maize starch and ETS as studied in ethanol. Bright field images showed the typical polygonal to

spherical shape of native maize starch granules (Eliasson, 2004). Native granules and ETS<sub>68%/95°C</sub> did not show outstanding morphological differences. Remarkably, the center of ETS<sub>58%/95°C</sub> granules contained small indentations. Such indentations were more pronounced for ETS<sub>53%/95°C</sub>. It appears that maize starch granules start to burst from the inside, where the hilum is situated, to the outside (Zhang, Dhital, Haque & Gidley, 2012). ETS<sub>48%/95°C</sub> had irregular shapes and indentations stretched across the entire granule. Under polarized light, native maize starch granules showed the typical Maltese cross pattern resulting from the long-range radial ordering of starch molecules (French, 1984). Again, ETS<sub>68%/95°C</sub> granules were microscopically quite similar to native starch. ETS<sub>58%/95°C</sub> and ETS<sub>53%/95°C</sub> had more diffuse birefringence patterns. Finally, ETS<sub>48%/95°C</sub> no longer contained the typical birefringence pattern of native starch. Instead, its granules showed a homogeneous weaker birefringence and Maltese cross patterns could hardly be observed.

### *3.1.3 Compositional changes due to aqueous ethanol treatment*

Table 1 lists AM and lipid contents of native starch and ETS. All ETS had a slightly lower AM content than native maize starch, but differences amongst ETS were not significant. Apparently, some AM leaching occurs during heating in aqueous ethanol. However, compared to native maize starch, a decrease in AM content reading of maximally 1.5% (ETS<sub>48%/95°C</sub>) was noted, which is rather low compared to literature data. Jane *et al.* (1986a) reported a decrease in AM content by 4.8% and 1.7% for granular cold-water swelling maize and wheat starches, respectively, when produced by method I. As can be expected, the present aqueous alcohol treatment results in partial defatting (Table 1) since heating starch in polar solvents allows lipid extraction (Pareyt, Finnie, Putseys & Delcour, 2011). More lipids were lost when ethanol concentration increased during the treatment. This was also evidenced by the decrease in  $\Delta H_{AML}$ . A small endotherm (0.8 J/g) at approximately 100 °C could be observed for native starch heated in excess water, which is characteristic for melting of naturally occurring AML present in native non-waxy starches (Morrison, Law & Snape, 1993). For ETS, this melting

endotherm decreased in size with increasing ethanol concentrations and eventually vanished for ETS<sub>68%/95°C</sub>.

#### *3.1.4 Swelling properties*

In deionized water (Figure 2, panels F1 and F2), ETS<sub>48%/95°C</sub> granules did swell to several times their initial size and birefringence was completely lost, suggesting immediate loss of molecular ordering when such starch comes in contact with water. Table 2 lists SP, C\* and CHL values at 20 °C. SP and CHL increased and C\* decreased in the order ETS<sub>68%/95°C</sub>, ETS<sub>58%/95°C</sub>, ETS<sub>53%/95°C</sub> to ETS<sub>48%/95°C</sub>, along with ETS showing a decreased level of remaining Maltese cross pattern. Compared to native maize starch (SP = 2.6 g/g; C\* = 39.0%) approximately a four-fold increase in SP (10.0 g/g) and similar decrease in C\* (10.4%) were noted for ETS<sub>48%/95°C</sub>.

#### *3.1.5 Crystalline structure*

Figure 3 shows WAXD patterns of native and ETS. Native maize starch showed the A-type diffraction pattern characteristic for cereal starches with intensity maxima at 14.9, 16.9, 17.6 and 22.7° 2 $\theta$ . It had a degree of crystallinity of 29%, 27% of which were A-type crystals. A broad reflection at approximately 19.5° 2 $\theta$  was responsible for the 2% V<sub>H</sub>-type crystallinity. This reflection has been associated with V-type AM (Cheetham & Tao, 1998) and its presence in the diffraction pattern of native maize starch can be explained by the natural occurrence of AML in native non-waxy cereal starches (Morrison, Law & Snape, 1993). Native starch and ETS<sub>68%/95°C</sub> showed approximately the same degree of crystallinity (30%) and proportions of A- (28%) and V<sub>H</sub>-type (2%) crystals. The latter starch still had the original Maltese cross pattern and no cold-water swelling properties. A gradual conversion from an A- to a V<sub>H</sub>-type diffraction pattern was observed in the order ETS<sub>58%/95°C</sub>, ETS<sub>53%/95°C</sub> to ETS<sub>48%/95°C</sub>. For ETS<sub>58%/95°C</sub>, which had only partial cold-water swelling properties, reflections emerged at 7.4, 12.8, 19.5 and 22.1° 2 $\theta$  characteristic for V<sub>H</sub>-type crystalline structures. It was composed of 21% A- and 12% V<sub>H</sub>-type crystals, together responsible for a crystallinity of 33%. The V<sub>H</sub>-type crystallinity (17%)

became dominant for ETS<sub>53%/95°C</sub>, although some A-type crystals (4%) remained. ETS<sub>48%/95°C</sub> had a crystallinity of 18%, with the crystals being only of the V<sub>H</sub>-type. For regular maize starch at a treatment temperature of 95 °C, some water:ethanol ratios still allow the original A-type crystals to melt completely without loss of the granular structure. The structural preservation seems to be facilitated by replacing the original A-type by V<sub>H</sub>-type crystals. The gradual changeover from an A- to a V<sub>H</sub>-type diffraction pattern in the production of GCWSS follows the conversion from granules with a Maltese cross pattern to granules with a hazy birefringence.

### 3.2 On the effect of alcohol removal on cold-water swelling properties

The effect of high temperature alcohol removal on the crystalline structure and swelling properties was studied by drying ETS<sub>48%/95°C</sub> at 115 °C, since TGA measurements of ETS<sub>48%/95°C</sub> showed the residual solvent to be completely removed at 115 °C (Figure 4). ETS<sub>48%/95°C</sub> oven-dried at 115 °C showed a V<sub>A</sub>-type diffraction pattern (Le Bail, Bizot, Pontoire & Buleon, 1995) with a degree of crystallinity of 22%, which evidently was higher than that of ETS<sub>48%/95°C</sub> dried at RT, which had a V<sub>H</sub>-type diffraction pattern and a crystallinity of 18% (*cf. supra*). Preferential removal of water from the amorphous fraction decreased the area of the amorphous halo and thus increased the relative weight of the crystalline portion and hence also the degree of crystallinity. However, after equilibration in a humidifier to approximately 16% final moisture content, the initial V<sub>H</sub>-type diffraction pattern with a degree of crystallinity of 18% was obtained again. SP and C\* of ETS<sub>48%/95°C</sub>, dried either at 115 °C or RT did not differ significantly (Table 2). These results prove that a high temperature drying step is not necessary to impart GCWSS with cold-water swelling properties. Still, the present study does not allow making definite conclusions regarding the question whether or not ethanol is located in the single helix cavity. However, when present in the cavity it would most likely be freely exchangeable with water (Brisson, Chanzy & Winter, 1991) and would not affect cold-water swelling ability.



### 3.3 On the thermal requirements for producing granular cold-water swelling maize starch

Figure 5 shows DSC thermograms of maize starch heated in different ethanol:water mixtures. Table 3 presents the corresponding gelatinization characteristics. As a control, the thermogram of maize starch gelatinized in pure water is shown (curve 5A). Heating in 48% (v/v) ethanol showed a sharp gelatinization endotherm occurring at higher temperatures than native starch gelatinized in pure water. With increasing ethanol concentrations, gelatinization took place at increasingly higher temperatures and over a broader temperature range. Moreover, the sharp gelatinization peak (G) obtained for heating in pure water or 48% ethanol was gradually transformed in a broader peak with a tailing shoulder (M1). In literature, these events have been associated with gelatinization of starch in progressively more limiting water conditions (Donovan, 1979). The G-endotherm has been attributed to dissociation of helices (loss of AP crystals) and the M1-endotherm to AP helix-coil transition (unwinding of AP double helices) (Waigh, Gidley, Komanshek & Donald, 2000). In excess water, these transitions are assumed to occur simultaneously and give rise to one sharp DSC endotherm (Waigh, Gidley, Komanshek & Donald, 2000). Hence, from the DSC thermograms in Figure 5 one can deduce that, in the case of 48% (v/v) ethanol, the ‘excess water’ condition – or more suitably, the ‘excess plasticizer’ condition – is still fulfilled. However, an increase in  $\Delta H$  and gelatinization temperature was observed compared to the situation in pure water (Table 3). This was attributed to 48% (v/v) ethanol:water being a less efficient plasticizer than pure water (Tan, Wee, Sopade & Halley, 2004). With increasing ethanol concentration [53 and 58% (v/v) ethanol], the G-endotherm decreased in size while the M1-endotherm gained importance. These changes were accompanied by further increases in gelatinization temperature and decreases in  $\Delta H$ . Under these circumstances, starch is gelatinized in limiting water conditions. The temperature at which the AP helix-coil transition takes place is higher than the temperature for the dissociation of AP double helices (Waigh, Gidley, Komanshek & Donald, 2000). Hence, both occur as separate thermal events. Eventually, the M1-endotherm becomes the only peak observable for

gelatinization in 68% (v/v) ethanol. A direct helix to coil transition has been said to occur at low water contents (Waigh, Gidley, Komanshek & Donald, 2000). Note that it is clear from these curves that loss of native molecular organization in water:ethanol mixtures with an ethanol concentration exceeding 48% (v/v), proceeds at temperatures above 95 °C, resulting in remaining A-type crystals when GCWSS is created at 95 °C as shown earlier (*cf.* §3.1.5).

We did not observe exothermic signals accounting for formation of V<sub>H</sub>-type crystals due to coincidence of A-type crystal melting and V<sub>H</sub>-type crystal formation in the same temperature interval (Jane, Craig, Seib & Hosney, 1986b). The high temperature melting endotherms in Figure 5 could be assigned to melting of created V<sub>H</sub>-type crystals. For increasing ethanol concentration, T<sub>P(V)</sub> increased and ΔH<sub>(V)</sub> decreased. These observations probably originated from solvents effects. Hence, the properties of the created V<sub>H</sub>-type crystals were studied with X-ray diffraction (*cf. infra*). Furthermore, the ΔT<sub>(V)</sub> became more narrow with increasing ethanol concentrations from 48 to 58% (v/v) and broadened again in the case of 68% (v/v) ethanol. Different solvents used induced different morphological features in V<sub>H</sub>-type crystals, impacting their thermal stability range. To fully elucidate this, time-temperature resolved X-ray data would be needed.

DSC thermograms in Figure 5 formed the basis for small scale production of GCWSS (*cf.* §2.9). Treatment temperatures were chosen with the rationale that gelatinization should be finished, whilst V<sub>H</sub>-type crystal melting should be prevented. Bright field microscopy images of ETS<sub>53%/107°C</sub>, ETS<sub>58%/112°C</sub> and ETS<sub>68%/133°C</sub> in ethanol (Figure 2, panel G1, I1 and K1) revealed similar deformations earlier noted for ETS<sub>48%/95°C</sub>. However, indentations became more confined to the granule center in the order ETS<sub>53%/107°C</sub> to ETS<sub>68%/133°C</sub>. Polarized optical microscopy (Figure 2, panel G2, I2 and K2) revealed a hazy birefringence with some remnants of Maltese cross patterns. These observations suggest that diffusion of starch molecules, more specifically the AM fraction (*cf.* §3.4), throughout the granule is limited with increasing ethanol concentrations, (partially) maintaining original molecular ordering. Microscopy images in water

(Figure 2, panel H, J and L) showed that these treatments had resulted in starches with cold-water swelling properties. Similar to ETS<sub>48%/95°C</sub>, ETS<sub>53%/107°C</sub>, ETS<sub>58%/112°C</sub> and ETS<sub>68%/133°C</sub> showed pure V<sub>H</sub>-type diffraction patterns (Figure 3, panel H, I and J) with a degree of crystallinity of 14, 12 and 16% respectively. Note that the scattering patterns of GCWSS produced on a mg scale showed increased noisiness, which hampered drawing solid conclusions on the degree of crystallinity. Since there was no obvious decreasing trend in V<sub>H</sub>-type crystallinity with increasing ethanol concentration, the decrease in  $\Delta H_{(V)}$  mentioned above (Figure 5, Table 3) was most likely due to a solvent effect. We can conclude that studying the thermal transitions of starch heated in different water:ethanol mixtures allows identifying a treatment temperature resulting in the conversion of native to V<sub>H</sub>-type GCWSS.

### 3.4 On the contribution of amylopectin in V<sub>H</sub>-type crystal formation

The AM and AP fractions have been assigned equal importance in V<sub>H</sub>-type crystal formation during production of GCWSS by method I (Jane, Craig, Seib & Hosney, 1986b). However, this was concluded based on comparison with the X-ray diffraction pattern of a V-type reference sample, which results in relative rather than absolute values for degree of crystallinity. In the present study, the degree of crystallinity of ETS<sub>48%/95°C</sub>, which had an AM content of 22% and contained V<sub>H</sub>-type crystals only, was 18%. Taken together with the fact that it is impossible to produce a granular cold-water swelling version of a waxy starch with a V<sub>H</sub>-type crystalline structure, this strongly suggests that AM is mainly responsible for V<sub>H</sub>-type crystal formation. This was further investigated by studying the crystalline structure and thermal properties of ETS<sub>waxy56%/95°C</sub>, which can be considered partially cold-water swelling based on its reduced post-treatment gelatinization enthalpy in excess water (Figure 1). WAXD experiments showed that indeed only 30% (Figure 3L) of the initially 43% A-type crystals (Figure 3K) remained. A small peak at 19.5 °2 $\theta$  was responsible for a V<sub>H</sub>-type crystallinity of 2%. However, DSC thermograms of heating waxy maize starch in 56% (v/v) ethanol did not reveal a V-type crystal melting endotherm (Figure 5, curve F), most likely since the signal is too small or overlaps with

436 the gelatinization endotherm. Either way, it is clear that the AM fraction is responsible for  
437 preservation of granular integrity by formation of stable V<sub>H</sub>-type crystals.

438

## CONCLUSIONS

At a temperature of 95 °C and ethanol concentration of 48% (v/v), the present aqueous ethanol procedure resulted in GCWSS. Its intact granules had V<sub>H</sub>-type crystals and birefringence when studied in ethanol under polarized light. Removal of alcohol by high temperature drying yielded a V<sub>A</sub>-type X-ray diffraction pattern. This transition was reversible upon exposure to high moisture conditions and high temperature drying was not necessary to impart GCWSS with cold-water swelling capacity. Regular GCWSS that contained 22% AM showed a degree of crystallinity of 18%. Reinforced by the current and past observations that complete conversion of waxy maize starch to a GCWSS with a V<sub>H</sub>-type crystalline structure is impossible, it can be concluded that the AM fraction is almost exclusively responsible for V<sub>H</sub>-type crystal formation. *In situ* calorimetric measurements provided insights into the thermal conditions needed to produce GCWSS from different ethanol:water mixtures. For progressively increasing ethanol concentrations, native A-type crystal melting occurred at higher temperatures and melting behavior was similar to that of starch gelatinized under progressively more limiting water conditions. A high temperature melting endotherm could be attributed to melting of created V<sub>H</sub>-type crystals. For ethanol concentrations exceeding 48% (v/v), higher treatment temperatures that ensured completion of native crystal melting but still prevented V<sub>H</sub>-type crystal melting effectively resulted in V<sub>H</sub>-type crystalline GCWSS.

## ACKNOWLEDGEMENTS

The Fonds Wetenschappelijk Onderzoek – Vlaanderen (FWO) is thanked for financial support. Technical assistance by Luc Van Den Ende and MSc. Maja Vanhalle is gratefully appreciated. Special thanks are offered to MSc. Andrés F. Doblado-Maldonado and Dr. Jung-Sun Hong for fruitful discussions. This work is part of the Methusalem programme ‘Food for the future’ (2007 – 2014). Jan A. Delcour is W.K. Kellogg Chair in Cereal Science and Nutrition at the KU Leuven. The authors thank the Hercules Foundation for supporting the purchase of equipment through the project AKUL/09/0035, Molybdenum high-energy X-ray source for *in situ* diffraction studies of advanced materials and single crystals.

- 469 Anastasiades, A., Thanou, S., Loulis, D., Stapatoris, A., & Karapantsios, T. D. (2002). Rheological  
470 and physical characterization of pregelatinized maize starches. *Journal of Food Engineering*, 52(1),  
471 57-66.
- 472 Brisson, J., Chanzy, H., & Winter, W. T. (1991). The crystal and molecular -structure of Vh  
473 amylose by electron-diffraction analysis. *International Journal of Biological Macromolecules*,  
474 13(1), 31-39.
- 475 Buléon, A., Colonna, P., Planchot, V., & Ball, S. (1998). Starch granules: structure and  
476 biosynthesis. *International Journal of Biological Macromolecules*, 23(2), 85-112.
- 477 Cairns, P., Bogracheva, T. Y., Ring, S. G., Hadley, C. L., & Morris, V. J. (1997). Determination of  
478 the polymorphic composition of smooth pea starch. *Carbohydrate Polymers*, 32(3-4), 275-282.
- 479 Cheetham, N. W. H., & Tao, L. P. (1998). Variation in crystalline type with amylose content in  
480 maize starch granules: an X-ray powder diffraction study. *Carbohydrate Polymers*, 36(4), 277-284.
- 481 Chen, J., & Jane, J. (1994a). Preparation of granular cold-water soluble starches by alcoholic  
482 alkaline treatment. *Cereal Chemistry*, 71(6), 618-622.
- 483 Chen, J., & Jane, J. (1994b). Properties of granular cold-water soluble starches prepared by  
484 alcoholic alkaline treatments. *Cereal Chemistry*, 71(6), 623-626.
- 485 Colonna, P., Doublier, J. L., Melcion, J. P., Demonredon, F., & Mercier, C. (1984). Extrusion  
486 cooking and drum drying of wheat starch. 1. Physical and macromolecular modifications. *Cereal*  
487 *Chemistry*, 61(6), 538-543.
- 488 Donovan, J. W. (1979). Phase-transitions of the starch-water system. *Biopolymers*, 18(2), 263-275.
- 489 Doublier, J. L., Colonna, P., & Mercier, C. (1986). Extrusion cooking and drum drying of wheat-  
490 starch. 2. Rheological characterization of starch pastes. *Cereal Chemistry*, 63(3), 240-246.
- 491 Dubois, M., Gilles, K. A., Hamilton, J. K., Rebers, P. A., & Smith, F. (1956). Colorimetric method  
492 for determination of sugars and related substances. *Analytical Chemistry*, 28(3), 350-356.
- 493 Eastman, J. E., 1987. Cold water swelling starch composition. U.S. patent 4,634,596.
- 494 Eastman, J. E., & Moore, C. O., 1984. Cold-water-soluble granular starch for gelled food  
495 compositions. U.S. patent 4,465,702.
- 496 Eerlingen, R. C., Jacobs, H., Block, K., & Delcour, J. A. (1997). Effects of hydrothermal treatments  
497 on the rheological properties of potato starch. *Carbohydrate Research*, 297(4), 347-356.
- 498 Eliasson, A. (2004). *Starch in food. Structure, function and applications*. Abington, Cambridge,  
499 England: Woodhead Publishing Limited.
- 500 French, A. D., & Murphy, V. G. (1977). Computer modeling in study of starch. *Cereal Foods*  
501 *World*, 22(2), 61-70.

502 French, D. (1984). Organization of starch granules. In R. L. Whistler, J. N. BeMiller & E. F.  
 503 Paschall (Eds.). *Starch: chemistry and technology* (pp. 183-247). New York, USA: Academic Press.  
 504 Gerits, L. R., Pareyt, B., & Delcour, J. A. (2013). Single run HPLC separation coupled to  
 505 evaporative light scattering detection unravels wheat flour endogenous lipid redistribution during  
 506 bread dough making. *Lwt-Food Science and Technology*, 53(2), 426-433.  
 507 Gibson, T. S., Solah, V. A., & McCleary, B. V. (1997). A procedure to measure amylose in cereal  
 508 starches and flours with concanavalin A. *Journal of Cereal Science*, 25(2), 111-119.  
 509 Gommers, C. J., & Goderis, B. (2010). CONEX, a program for angular calibration and averaging of  
 510 two-dimensional powder scattering patterns. *Journal of Applied Crystallography*, 43, 352-355.  
 511 Imberty, A., Chanzy, H., Perez, S., Buleon, A., & Tran, V. (1988). The double-helical nature of the  
 512 crystalline part of A-starch. *Journal of Molecular Biology*, 201(2), 365-378.  
 513 Imberty, A., & Perez, S. (1988). A revisit to the 3-dimensional structure of B-type starch.  
 514 *Biopolymers*, 27(8), 1205-1221.  
 515 Jane, J., Craig, S. A. S., Seib, P. A., & Hosney, R. C. (1986a). Characterization of granular cold  
 516 water-soluble starch. *Starch-Starke*, 38(8), 258-263.  
 517 Jane, J. L., Craig, S. A. S., Seib, P. A., & Hosney, R. C. (1986b). A granular cold water-soluble  
 518 starch gives a V-type X-ray diffraction pattern. *Carbohydrate Research*, 150(1), C5-C6.  
 519 Jane, J. L., & Seib, P. A., 1991. Preparation of granular cold water swelling soluble starches by  
 520 alcoholic-alkali treatments. U.S. patent 5,057,157.  
 521 Jenkins, J. P. J., Cameron, R. E., & Donald, A. M. (1993). A universal feature in the structure of  
 522 starch granules from different botanical sources. *Starch-Starke*, 45(12), 417-420.  
 523 Le Bail, P., Bizot, H., Pontoire, B., & Buleon, A. (1995). Polymorphic transitions of amylose-  
 524 ethanol crystalline complexes induced by moisture exchanges. *Starch-Starke*, 47(6), 229-232.  
 525 Leach, H. W., McCowen, L. D., & Schoch, T. J. (1959). Structure of the starch granule. 1. Swelling  
 526 and solubility patterns of various starches. *Cereal Chemistry*, 36(6), 534-544.  
 527 Morrison, W. R., Law, R. V., & Snape, C. E. (1993). Evidence for inclusion complexes of lipids  
 528 with V-Amylose in maize, rice and oat Starches. *Journal of Cereal Science*, 18(2), 107-109.  
 529 Oostergetel, G. T., & Vanbruggen, E. F. J. (1989). On the origin of a low-angle spacing in starch.  
 530 *Starch-Starke*, 41(9), 331-335.  
 531 Pareyt, B., Finnie, S. M., Putseys, J. A., & Delcour, J. A. (2011). Lipids in bread making: sources,  
 532 interactions, and impact on bread quality. *Journal of Cereal Science*, 54(3), 266-279.  
 533 Pitchon, E., O'Rourke, J. D., & Joseph, T. H., 1981. Process for cooking or gelatinizing materials.  
 534 U.S. patent 4,280,851.  
 535 Rajagopalan, S., & Seib, P. A. (1992a). Granular cold-water-soluble starches prepared at  
 536 atmospheric-pressure. *Journal of Cereal Science*, 16(1), 13-28.



537 Rajagopalan, S., & Seib, P. A. (1992b). Properties of granular cold-water-soluble starches prepared  
538 at atmospheric-pressure. *Journal of Cereal Science*, 16(1), 29-40.

539 Saibene, D., & Seetharaman, K. (2010). Amylose involvement in the amylopectin clusters of potato  
540 starch granules. *Carbohydrate Polymers*, 82(2), 376-383.

541 Tan, I., Wee, C. C., Sopade, P. A., & Halley, P. J. (2004). Investigation of the starch gelatinisation  
542 phenomena in water-glycerol systems: application of modulated temperature differential scanning  
543 calorimetry. *Carbohydrate Polymers*, 58(2), 191-204.

544 Waigh, T. A., Gidley, M. J., Komanshek, B. U., & Donald, A. M. (2000). The phase  
545 transformations in starch during gelatinisation: a liquid crystalline approach. *Carbohydrate*  
546 *Research*, 328(2), 165-176.

547 Whittam, M. A., Orford, P. D., Ring, S. G., Clark, S. A., Parker, M. L., Cairns, P., & Miles, M. J.  
548 (1989). Aqueous dissolution of crystalline and amorphous amylose alcohol complexes.  
549 *International Journal of Biological Macromolecules*, 11(6), 339-344.

550 Zhang, B. S., Dhital, S., Haque, E., & Gidley, M. J. (2012). Preparation and characterization of  
551 gelatinized granular starches from aqueous ethanol treatments. *Carbohydrate Polymers*, 90(4),  
552 1587-1594.

553 Zobel, H. F. (1988). Starch crystal transformations and their industrial importance. *Starch-Starke*,  
554 40(1), 1-7.

555

556

557

558

Tables

559 **Table 1:** Amylose and lipid contents of native maize starch and ethanol treated starches (ETS) made at 95 °C using  
560 different treatment concentrations of ethanol (v/v). Corresponding amylose-lipid inclusion complex melting enthalpies  
561 ( $\Delta H_{AML}$ ) are also listed.

Sample	Amylose (% dm)	Lipids (% dm)	$\Delta H_{AML}$ (J/g dm)
native maize	23.7 (0.4) <sup>a</sup>	0.19 (0.02) <sup>a</sup>	0.8 (0.1) <sup>a</sup>
ETS <sub>68%/95°C</sub>	22.8 (0.4) <sup>b</sup>	0.03 (0.01) <sup>b</sup>	n.d.
ETS <sub>58%/95°C</sub>	22.9 (0.1) <sup>b</sup>	0.05 (0.00) <sup>b</sup>	0.1 (0.0) <sup>b,c</sup>
ETS <sub>53%/95°C</sub>	22.4 (0.7) <sup>b</sup>	0.10 (0.03) <sup>c</sup>	0.2 (0.1) <sup>b,c</sup>
ETS <sub>48%/95°C (RT)</sub>	22.2 (0.3) <sup>b</sup>	0.14 (0.02) <sup>c</sup>	0.2 (0.1) <sup>c</sup>

562 Results in the same column indicated with the same letter are not significantly different ( $P < 0.05$ ).  
563 n.d.: not detectable.

564 **Table 2:** Swelling power (SP), close packing concentration ( $C^*$ ) and carbohydrate leaching (CHL) at 20 °C of native  
565 maize starch and ethanol treated starches (ETS) made at 95 °C using different treatment concentrations of ethanol (v/v).  
566 For ETS<sub>48%/95°C</sub>, results are given for regular air-drying overnight (ETS<sub>48%/95°C</sub>) and high temperature drying for 60 min  
567 at 115 °C (ETS<sub>48%/95°C\_115°C</sub>).

Sample	SP (g/g)	$C^*$ (%)	CHL (%)
native maize	2.6 (0.1) <sup>a</sup>	39.0 (1.5) <sup>a</sup>	n.d.
ETS <sub>68%/95°C</sub>	2.8 (0.2) <sup>a</sup>	35.8 (2.8) <sup>a</sup>	n.d.
ETS <sub>58%/95°C</sub>	3.7 (0.1) <sup>b</sup>	27.3 (0.7) <sup>b</sup>	0.3 (0.0) <sup>b</sup>
ETS <sub>53%/95°C</sub>	7.4 (0.3) <sup>c</sup>	13.7 (0.5) <sup>c</sup>	1.8 (0.2) <sup>c</sup>
ETS <sub>48%/95 °C</sub>	10.6 (0.2) <sup>d</sup>	9.9 (0.1) <sup>d</sup>	5.7 (0.1) <sup>d</sup>
ETS <sub>48%/95°C_115°C</sub>	10.4 (0.0) <sup>d</sup>	10.1 (0.0) <sup>d</sup>	5.7 (0.1) <sup>d</sup>

568 Results in the same column indicated with the same letter are not significantly different ( $P < 0.05$ ).  
569 n.d.: not detectable.

570 **Table 3:** Gelatinization and V-type crystal melting characteristics of native maize starch heated in ethanol: water  
571 mixtures containing different concentrations of ethanol (v/v). Peak temperatures of gelatinization ( $T_P$ ) and V-type  
572 crystal melting ( $T_{P(V)}$ ), enthalpies of gelatinization ( $\Delta H$ ) and V-type crystal melting ( $\Delta H_{(V)}$ ) and temperature ranges of  
573 gelatinization ( $\Delta T$ ) and V-type crystal melting ( $\Delta T_{(V)}$ ) are shown with standard deviations between brackets. As a  
574 control, the gelatinization characteristics of native maize starch heated in excess pure water in a high pressure steel pan  
575 are given as well.

Solvent	$T_P$ (° C)	$\Delta H$ (J/g dm)	$\Delta T$ (° C)	$T_{P(V)}$ (° C)	$\Delta H_{(V)}$ (J/g dm)	$\Delta T_{(V)}$ (° C)
Pure water	69.9 (0.1)	13.9 (0.1)	14.8 (0.4)	n.a.	n.a.	n.a.
68% (v/v) ethanol	117.1 (1.9)	7.3 (0.2)	22.8 (1.0)	157.4 (0.4)	1.6 (0.1)	20.4 (0.9)
58% (v/v) ethanol	92.2 (0.7)	9.7 (1.0)	22.7(0.7)	140.4 (1.5)	3.9 (0.1)	12.2 (0.6)
53% (v/v) ethanol	87.6 (0.2)	11.8 (1.5)	20.7 (1.5)	129.5 (0.4)	4.1 (0.4)	15.6 (1.5)
48% (v/v) ethanol	82.3 (0.8)	15.2 (0.4)	15.0 (0.4)	117.6 (2.1)	4.5 (0.2)	27.3 (2.0)

576 n.a.: not applicable.

## 577 **Figure captions**

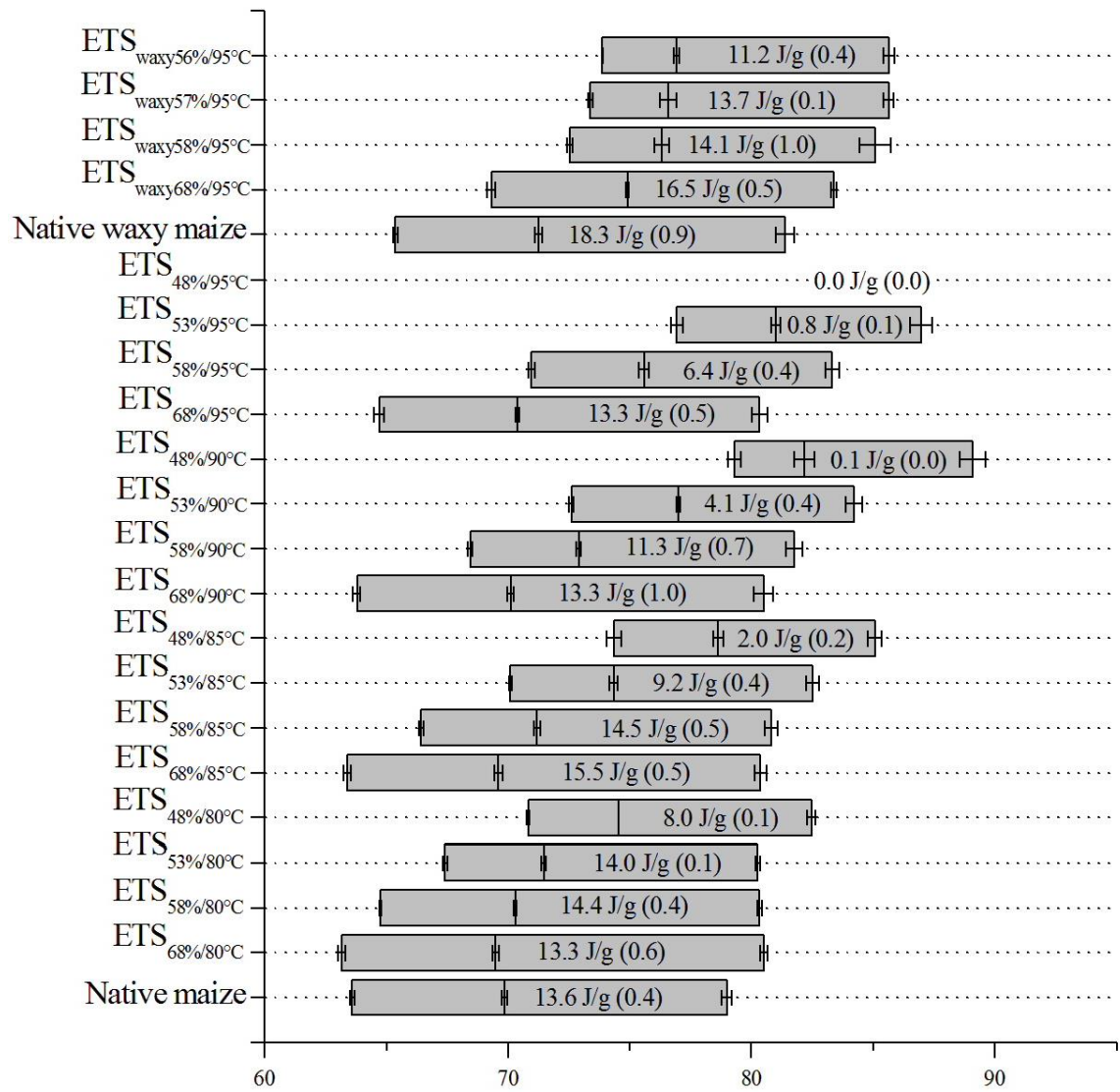
578 **Figure 1:** Schematic overview of the gelatinization characteristics of native and ethanol treated starches (ETS). The  
579 subscript 'waxy' refers to waxy maize starch. Different treatment concentrations of ethanol (v/v) and treatment  
580 temperatures ( $^{\circ}\text{C}$ ) are indicated. Start and end points of the bars represent onset ( $T_{\text{O}}$ ) and conclusion ( $T_{\text{C}}$ ) temperatures  
581 of gelatinization. The vertical line inside the bar is the peak temperature of gelatinization ( $T_{\text{P}}$ ). Gelatinization enthalpies  
582 (J/g) are given with standard deviations between brackets.

583 **Figure 2:** Bright field (1) and polarized light (2) microscopy images as studied in ethanol (A-E, G, I, K) and deionized  
584 water (F, H, J, L) of native maize starch (A) and ethanol treated starch (ETS): ETS<sub>68%/95 $^{\circ}\text{C}$</sub>  (B), ETS<sub>58%/95 $^{\circ}\text{C}$</sub>  (C),  
585 ETS<sub>53%/95 $^{\circ}\text{C}$</sub>  (D), ETS<sub>48%/95 $^{\circ}\text{C}$</sub>  (E, F), ETS<sub>53%/107 $^{\circ}\text{C}$</sub>  (G, H), ETS<sub>58%/112 $^{\circ}\text{C}$</sub>  (I, J) and ETS<sub>68%/133 $^{\circ}\text{C}$</sub>  (K, L).

586 **Figure 3:** Wide-angle X-ray diffraction patterns of native and ethanol treated starch (ETS): native maize starch (A),  
587 ETS<sub>68%/95 $^{\circ}\text{C}$</sub>  (B), ETS<sub>58%/95 $^{\circ}\text{C}$</sub>  (C), ETS<sub>53%/95 $^{\circ}\text{C}$</sub>  (D), ETS<sub>48%/95 $^{\circ}\text{C}$</sub>  (E), ETS<sub>48%/95 $^{\circ}\text{C}$</sub>  dried at 115  $^{\circ}\text{C}$  without equilibration (F)  
588 and with equilibration to approximately 16% final moisture content (G), ETS<sub>53%/107 $^{\circ}\text{C}$</sub>  (H), ETS<sub>58%/112 $^{\circ}\text{C}$</sub>  (I), ETS<sub>68%/133 $^{\circ}\text{C}$</sub>   
589 (J), native waxy maize starch (K) and ETS<sub>waxy56%/95 $^{\circ}\text{C}$</sub>  (L). Experimentally obtained scattering patterns (open circles) are  
590 fitted with an appropriate proportioned combination of an amorphous (white), A-type (grey) and V<sub>H</sub>-type (black)  
591 crystalline scattering pattern using a least-squared error fit model. Amorphous, A- and V<sub>H</sub>-type crystalline proportions  
592 are indicated. The scattered intensities are given in arbitrary units (a.u.).

593 **Figure 4:** Thermal gravimetric analysis profile of ethanol treated starch (ETS) showing cold-water swelling properties  
594 (ETS<sub>48%/95 $^{\circ}\text{C}$</sub> ). Weight (%) (full line) and first derivative of weight (%/ $^{\circ}\text{C}$ ) (dotted line) are given as a function of  
595 temperature ( $^{\circ}\text{C}$ ).

596 **Figure 5:** Differential scanning calorimetry (DSC) profiles of maize starch heated in pure water (A), 48% (v/v) ethanol  
597 (B), 53% (v/v) ethanol (C), 58% (v/v) ethanol (D) and 68% (v/v) (E) ethanol. The DSC profile of waxy maize starch  
598 heated in 56% (v/v) (F) ethanol is also shown. Relevant thermal transitions that could be attributed to gelatinization (G  
599 and M<sub>1</sub>) and V-type crystal melting (V) are indicated with arrows.



601  
602 **Figure 1**

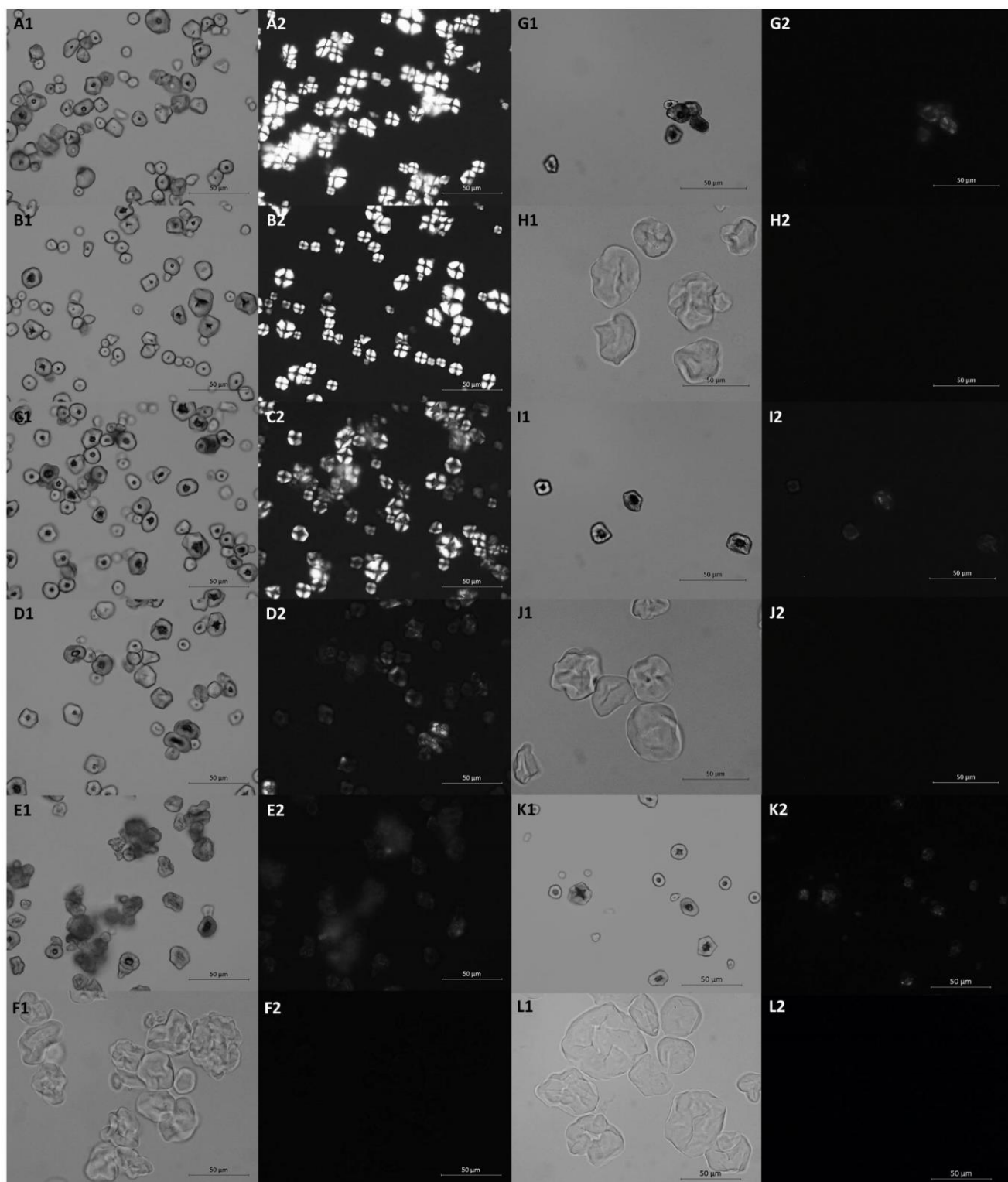


**Figure 2**

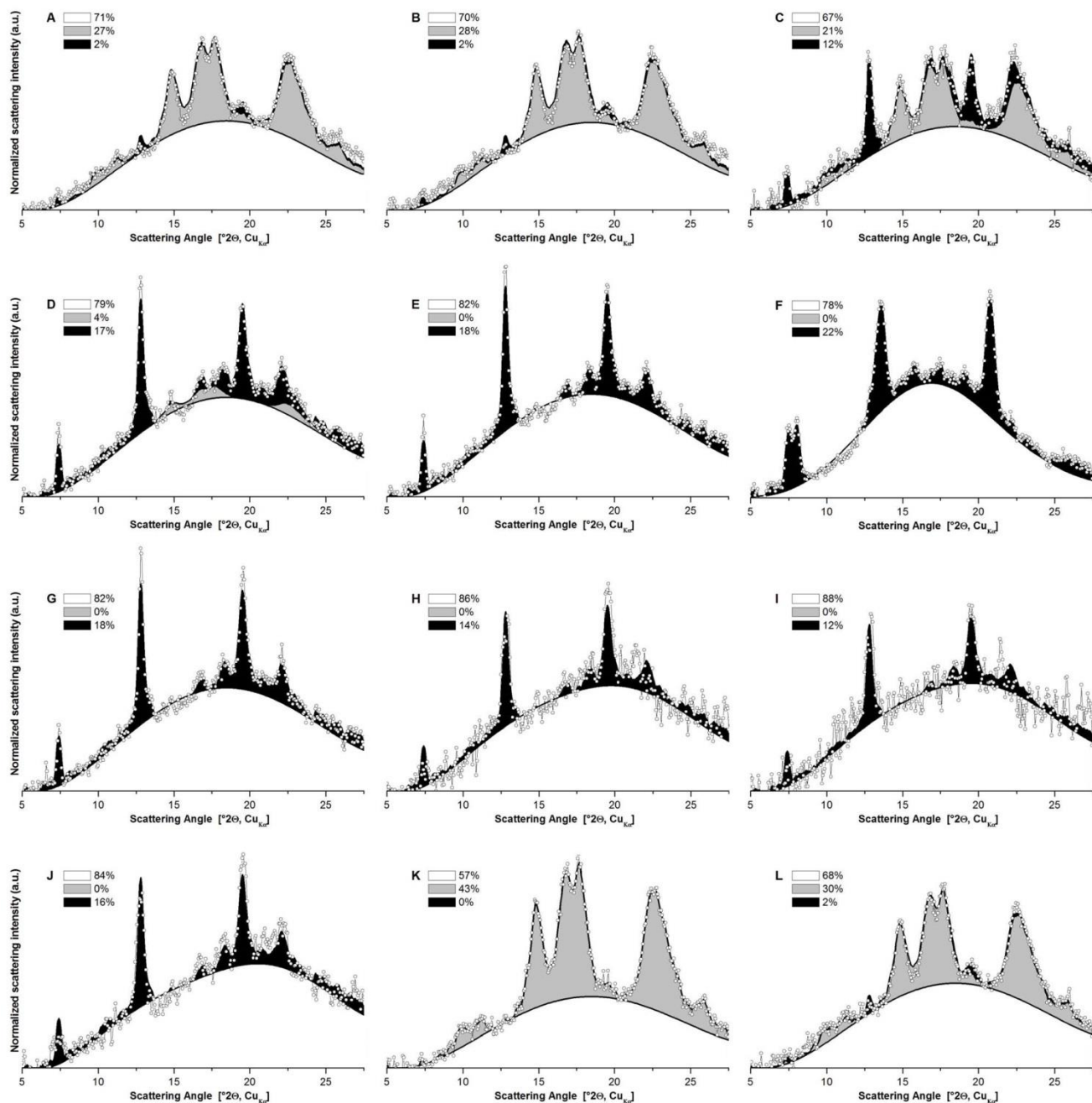
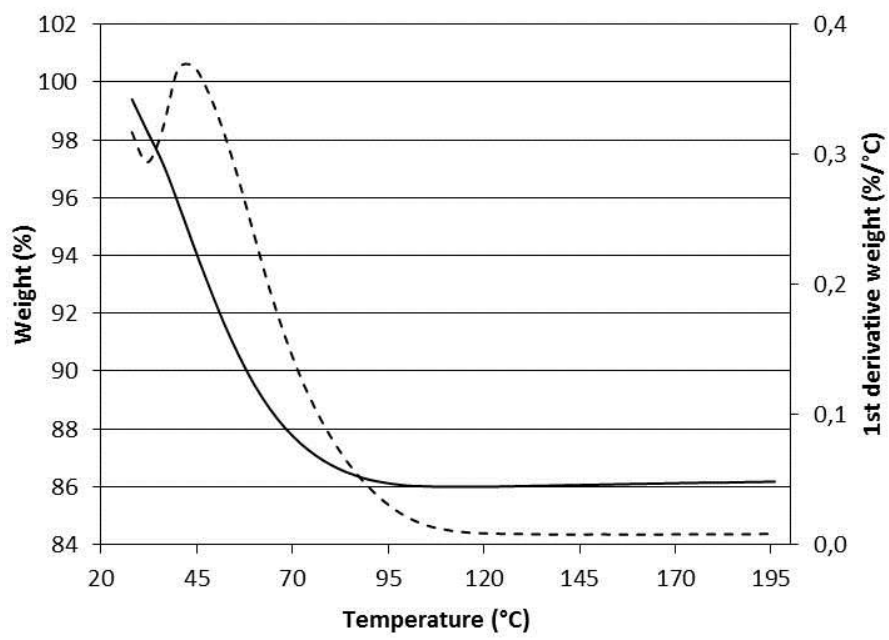


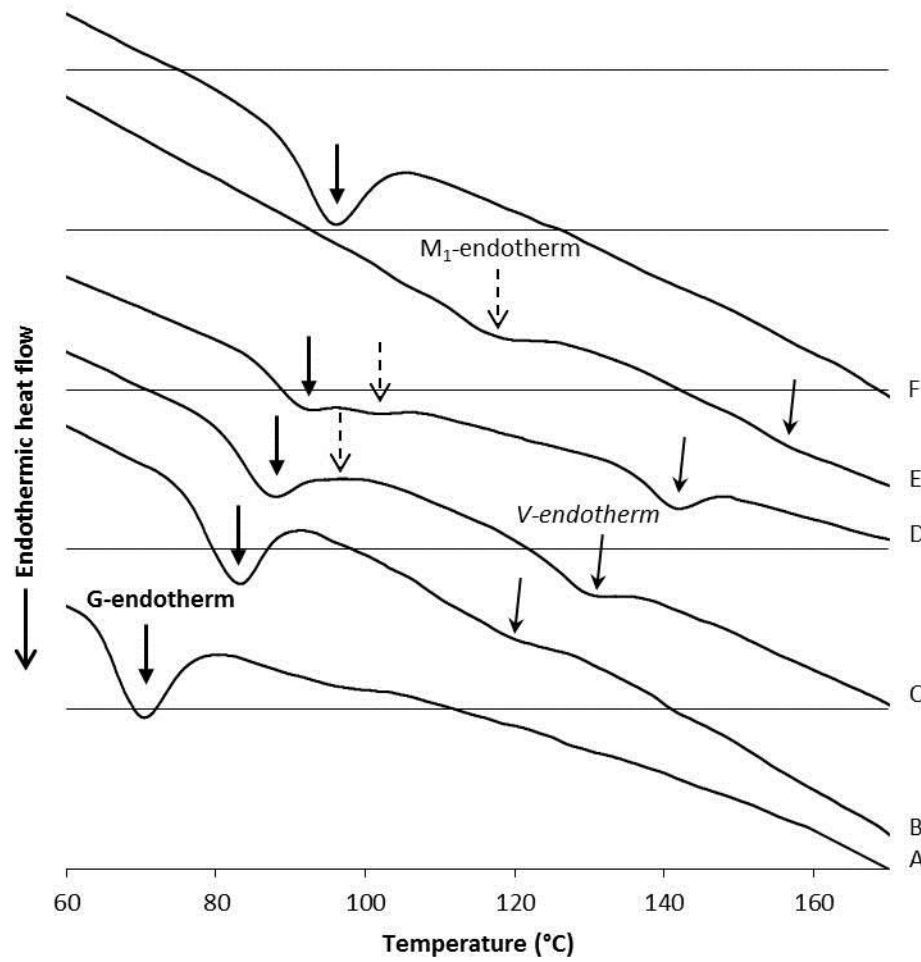
Figure 3

607



608

609 **Figure 4**



610

611 **Figure 5**

